When is a symmetric body-hinge structure isostatic?

Bernd Schulze*

Department of Mathematics and Statistics
University of Lancaster
Lancaster LA1 4YF, UK
Tel:44 (0) 1524 592173
Fax: 44 (0) 1524 592681
b.schulze@lancaster.ac.uk

Simon Guest

Department of Engineering
University of Cambridge
Trumpington Street, Cambridge CB2 1PZ, UK

Patrick W. Fowler

Department of Chemistry
University of Sheffield
Sheffield S3 7HF, UK

Abstract

A symmetry-extended mobility rule is formulated for body-hinge frameworks and used to derive necessary symmetry conditions for isostatic (statically and kinematically indeterminate) frameworks. Constructions for symmetric body-hinge frameworks with an isostatic scalar count are reported, and symmetry counts are used to examine these structures for hidden, symmetry-detectable mechanisms. Frameworks of this type may serve as examples for exploration of a symmetry extension of the (now proven) 'molecular conjecture'.

Keywords: symmetry, rigidity, isostatic, body-hinge structure, molecular

1. Introduction

Isostatic systems are both kinematically and statically determinate, and so are fixed in configuration, and have no internal stresses when unloaded, thus allowing high precision placement of components, as discussed by Maxwell for scientific apparatus in Section 4 of (Maxwell, 1876). This has particular engineering relevance in harsh thermal environments such as space (Bujakas and Rybakova, 1998). Isostatic systems are able to react to changes in shape of their constituent bodies by deforming without building up internal stresses, and so find application as 'parallel' robots, such as the Stewart platform (Stewart, 1965), deployable structures (Miura et al., 1985) and easily driven adaptive structures (Baker and Friswell, 2009)

In general, symmetry arguments give powerful tools for the detection of hidden mechanisms in structures that scalar counting arguments would predict to be isostatic. There are also many examples of highly symmetric structures that counting without symmetry predicts to be over-constrained, but which have mechanisms that are revealed by symmetry-extended counting rules (Röschel, 2002, 2012; Chen et al., 2012). The symmetry approach has already been used to develop symmetry-extended mobility criteria for bar-and-joint (Fowler and Guest, 2000; Connelly et al., 2009) and body-bar (Guest et al., 2010) frameworks. Here we make a natural extension to body-hinge structures, as a way of finding the symmetries of their mechanisms and

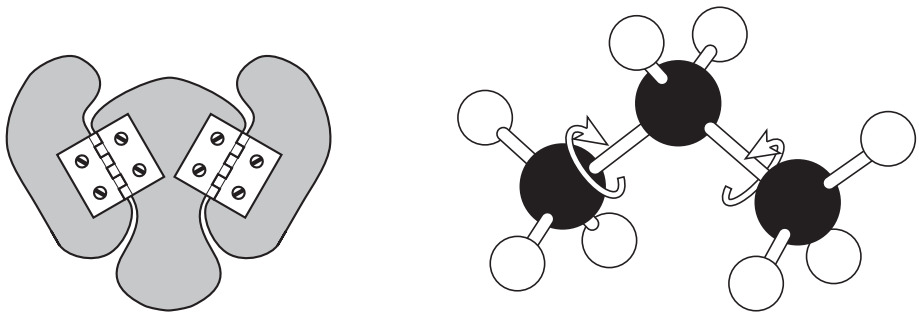

Figure 1: Two example body-hinge structures: (a) shows a central panel connected to two outer planes through simple rotational hinges; (b) shows a model of a propane molecule in which each of the outer methyl groups is able to rotate about the bond to the central carbon atom. Each of these structures has two mechanisms, as in each case the hinges are able to rotate independently of one another.

states of self stress and identifying conditions for a symmetric structure of this type to be isostatic. Two simple examples of body-hinge structures are shown in Figure 1

In addition to the practical goal of explaining mechanisms in particular systems, the study of symmetry aspects of body-hinge structures has another motivation. The long-standing 'molecular conjecture' (Tay and Whiteley, 1984) was recently proved (Katoh and Tanigawa, 2011): under generic conditions, a body-hinge framework and a 'molecular' structure with the same underlying multi-graph have the same rigidity properties. (A *molecular structure*, named by analogy with chemical structures, is one in which the lines of the hinges attached to each body all pass through a common point in that body. Figure 1(b) shows an example based on the propane molecule.)

A recently proposed generalisation is the conjecture that symmetric body-bar, body-hinge and molecular structures that all share a common symmetry

and a common underlying multi-graph will have the same rigidity properties under symmetry-generic conditions (Porta et al., 2013). Comparison of the analogous symmetry counts for body-bar frameworks and the molecular structures that result from specialisation of the body-hinge systems considered in the present study could provide extra evidence for the 'symmetric molecular conjecture'. The present study also gives ways of quickly constructing examples of symmetric molecular structures with small numbers of mechanisms, for comparison with corresponding body-bar frameworks, hence furnishing examples for investigation of the symmetric molecular conjecture.

The plan of the paper is as follows. First, the symmetry-extended mobility rule for body-hinge structures is obtained for assemblies of bodies pairwise connected by revolute hinges. Secondly, we derive general symmetry constraints on isostatic structures of body-hinge type. Finally, we present constructions for systems that are predicted to be isostatic by counting without symmetry, and examine their symmetry counts to determine whether they have symmetry-detectable mechanisms that are hidden by the scalar count.

In what follows, it is assumed that we are working with frameworks in three dimensions, except when specifically stated that we are dealing with the restriction of the system to the plane.

2. Background

The simple counting rule for calculating to first order the degrees of freedom (or the *mobility*) m of a mechanical linkage with b bodies connected by

g joints, where joint i permits f_i degrees of freedom, is associated with Grbler and Kutzbach and was given in the following form by Hunt(Hunt, 1978):

$$m = 6(b-1) - 6g + \sum_{i=1}^{g} f_i. \tag{1}$$

The generalized version of this rule that allows for states of self-stress in the same way as Calladine's extension (Calladine, 1978) of Maxwell's Rule for bar-and-joint frameworks (Maxwell, 1864) is

$$m - s = 6(b-1) - 6g + \sum_{i=1}^{g} f_i, \tag{2}$$

where s is the dimension of the space of self-stresses of the linkage. Equation 2 can be derived by considering the dimensions of the four fundamental vector subspaces of an equilibrium/compatability matrix, which can be defined for any set of linearised constraints (see, e.g., Guest and Pellegrino (1994) for an example).

A joint which allows exactly one revolute degree of freedom between the two bodies that it joins is called a *hinge*. Moreover, a mechanical linkage is called a *body-hinge structure* if every joint of the linkage is a hinge. Our goal is to derive necessary conditions for a symmetric body-hinge structure to be isostatic, i.e., to have $m = s = 0$.

Note that for a body-hinge structure with b bodies and h hinges, (2) becomes

$$m - s = 6(b-h-1) + h = 6b - 6 - 5h. \tag{3}$$

(In the restriction to two dimensions, the RHS is $3(b-h-1)+h = 3b-3-2h$.)

3. A symmetry-extended mobility rule for body-hinge structures

The symmetry-extended version of the generalized mobility rule (2) is (Guest and Fowler, 2005):

$$\Gamma(m) - \Gamma(s) = (\Gamma_T + \Gamma_R) \times (\Gamma(v, C) - \Gamma_{\|}(e, C) - \Gamma_0) + \Gamma_{\mathrm{f}} \qquad (4)$$

where each Γ is the vector of the traces of the corresponding representation matrices in some point group $\mathcal{G}$. Each such Γ is known in applied group theory as a *representation* of $\mathcal{G}$ (Bishop, 1973), or in mathematical group theory as a *character* (James and Liebeck, 2001). In applied group theory, the term character is often used informally for denoting an entry of a representation, i.e., the trace of a representation matrix (Cotton, 1990) for a given operation.

In (4), $\Gamma(m)$ and $\Gamma(s)$ are the representations of the mobility and the states of self-stress, respectively. Γ_T and Γ_R are the representations of rigid-body translations and rotations, and can be read off from standard character tables for point-groups (Atkins et al., 1970; Altmann and Herzig, 1994). In 3D, Γ_T+Γ_R is the six-dimensional $\Gamma(T_x, T_y, T_z)$+$\Gamma(R_x, R_y, R_z)$; in 2D, Γ_T+Γ_R is the three-dimensional $\Gamma(T_x, T_y) + \Gamma(R_z)$, where the system lies in the xy plane. Γ_0 denotes the trivial representation which takes the value of one for all group elements.

The other representations are defined in terms of the so-called *contact*

polyhedron C associated with the given body-hinge structure. C has one vertex for each body of the structure and two vertices are joined by an edge of C iff the corresponding bodies are connected by a joint. There is some choice in the construction of C, as we discuss further below. Note that C is not always a polyhedron in the graph theoretical sense: in some cases it may correspond to a non-planar graph, and in some to a non-planar graph. Further, its geometric embedding may have non-planar faces, or even degenerate to a polygon. $\Gamma(v, C)$ is the permutation representation of the vertices of C, and $\Gamma_{\|}(e, C)$ is the representation of a set of vectors along the edges of C. Finally, Γ_{f} is the representation of the total set of freedoms allowed by the joints.

Our previous treatments of mobility (Guest and Fowler, 2005) deals with hinges of all type including sliders and screws, but in the present context, for a body-hinge structure, the symmetry-extended mobility rule (Guest and Fowler, 2005) equivalent to (3) is

$$\Gamma(m) - \Gamma(s) = (\Gamma_T + \Gamma_R) \times (\Gamma(v, C) - \Gamma_{\|}(e, C) - \Gamma_0) + \Gamma_{\mathrm{h}} \qquad (5)$$

where Γ_{h} is the representation of the revolute degrees of freedom allowed by the hinges (which we will determine below).

The form of the product on the RHS of (5) has one immediate consequence: as the multiplier $(\Gamma_T + \Gamma_R)$ has character zero under all improper (parity reversing) operations, the character of $\Gamma(m) - \Gamma(s)$ under such op-

erations is determined entirely by that of the hinge freedoms for those operations. A second deduction can be made about frameworks that have an isostatic count of bars and hinges *and* have no body or hinge lying on an element of symmetry. Following the reasoning applied to bar-and-joint frameworks in (Fowler et al., 2014), in the present case it is the bodies and hinges that fall into *orbits* of size $|\mathcal{G}|$, and all vertex, edge and hinge representations are multiples of $\Gamma_{\rm reg}$ (which has character $|\mathcal{G}|$ under the identity, and zero under all other symmetry operations). Thus,

$$\begin{aligned} \Gamma(v,C) &= b_0\Gamma_{\rm reg} \\ \Gamma_{\parallel}(e,C) &= \Gamma_{\rm h} = h_0\Gamma_{\rm reg}, \end{aligned}$$

with $b_0 = b/|\mathcal{G}|$ and $h_0 = h/|\mathcal{G}|$. Since the framework has an isostatic count under the identity operation, we have (in 3D)

$$(6b_0 - 5h_0)|\mathcal{G}| = 6. \tag{6}$$

The full symmetry equation (5) reduces to

$$\Gamma(m) - \Gamma(s) = \frac{6}{|\mathcal{G}|}\Gamma_{\rm reg} - (\Gamma_T + \Gamma_R), \tag{7}$$

implying that the representation $\Gamma(m)-\Gamma(s)$ has character $-4\cos(2\pi/n) - 2$ under operations C_n, and zero under all others. The framework must then have symmetry-detectable mechanisms and/or states of self stress *unless* the

rigid body motions have the special symmetry

$$\Gamma_T + \Gamma_R = \frac{6}{|\mathcal{G}|}\Gamma_{\text{reg}}. \tag{8}$$

This last relation holds only for the following point groups: $\mathcal{C}_{3v}$, $\mathcal{C}_{3h}$, $\mathcal{S}_6$ ($|\mathcal{G}| = 6$); $\mathcal{C}_3$ ($|\mathcal{G}| = 3$); $\mathcal{C}_i$, $\mathcal{C}_s$ ($|\mathcal{G}| = 2$); and the trivial $\mathcal{C}_1$ ($|\mathcal{G}| = 1$). In all other groups, no framework where the count is isostatic and all components are general position can be isostatic in fact.

For frameworks restricted to the plane, equations (7) and (8) reduce to

$$\Gamma(m) - \Gamma(s) = \frac{3}{|\mathcal{G}|}\Gamma_{\text{reg}} - (\Gamma_T + \Gamma_R), \tag{9}$$

and the isostatic requirement is

$$\Gamma_T + \Gamma_R = \frac{3}{|\mathcal{G}|}\Gamma_{\text{reg}}. \tag{10}$$

The available point groups for the 2D case are $\mathcal{C}_n$ and $\mathcal{C}_{nv}$ (with $\mathcal{C}_s \equiv \mathcal{C}_{1v}$), and the requirement (10) holds *only* for $\mathcal{C}_3$ and the trivial $\mathcal{C}_1$. Thus, $\mathcal{C}_3$ is the only non-trivial symmetry group for which a 2D isostatic framework cab be achieved without structural elements lying on an element of symmetry.

The machinery of the symmetry-extended mobility rule requires a geometric realisation of the contact graph, and this is what we are calling here the contact polyhedron, C. The notion of a contact polyhedron requires some further discussion in the context of body-hinge frameworks. Given a body-

hinge assembly, the *contact graph* is defined by the underlying combinatorics of the assembly; the vertices correspond to the bodies and the edges to the hinges, each of which links exactly two bodies. Thus, the contact graph is simple, without loops or multiple edges. We are interested in the kinematics of this assembly, rather than the physical shapes of the individual bodies, and hence the significant geometrical information is that related to the positioning of the hinge lines. Together, the contact graph and the geometry of the hinge lines together define the 'kinematic symmetry' of the framework, and hence a point group $\mathcal{G}$.

In general, there is some freedom in the choice of the contact polyhedron C. To maximize information, we wish to work within the kinematic symmetry group, the largest point group compatible with the disposition of hinges and bodies, and therefore impose this symmetry on C. For simplicity, where possible we wish to align edges of C along hinge lines. Hinges which are aligned with edges of C will be called *torsional hinges*. In some cases, this alignment will fully define the positions of the vertices of C. If this is true for all vertices, and hence all hinges are torsional hinges, then we have a molecular framework, as defined earlier. Hinges that are not so aligned with edges will be called *non-torsional*. In frameworks confined to the plane, all hinges are of this type.

Figure 2 shows a simple case where two fully symmetric choices of C can be made, one where all edges of C line up with hinge lines (torsional) and one where all edges of C are perpendicular to hinge lines (non-torsional). Working

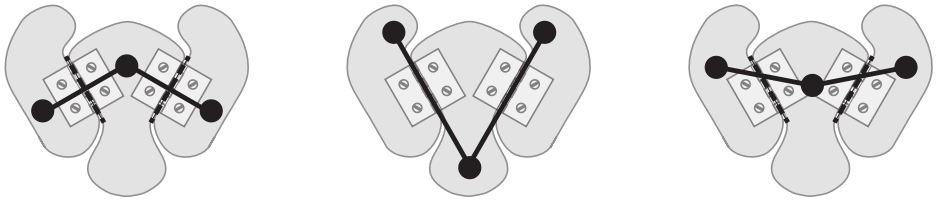

(a) (b) (c)

Figure 2: Examples of the choice of geometrically distinct contact 'polyhedra' for the same body-hinge structure, in this case the three plane structure shown in Figure 1(a). Three choices are shown: (a) edges chosen perpendicular to the hinge lines; (b) edges chosen along the hinge lines; (c) edges chosen to have no particular geometric relationship with the hinge lines.

consistently with either choice yields the same expression for $\Gamma(m)-\Gamma(s)$, as it must, since mechanisms and self-stresses exist independently of our procedure for calculating their representations. In this case, we find $\Gamma(m) - \Gamma(s) = A_2 + B_2$, which describe respectively con- and dis-rotatory combinations of the two independent hinge mechanisms.

4. Derivation of the symmetry representations for isostatic body-hinge frameworks

Given a choice of contact polyhedron, and in particular the positions of the edges, hinges fall into the two basic types, torsional and non-torsional, defined above and illustrated in Figures 3 and 4.

In order to apply the symmetry-extended mobility rule, we need to know how the degree of freedom of a hinge behaves under the various symmetry operations that might leave the hinge unshifted. For a given hinge, the contribution to the character (or trace of the representation matrix) for an

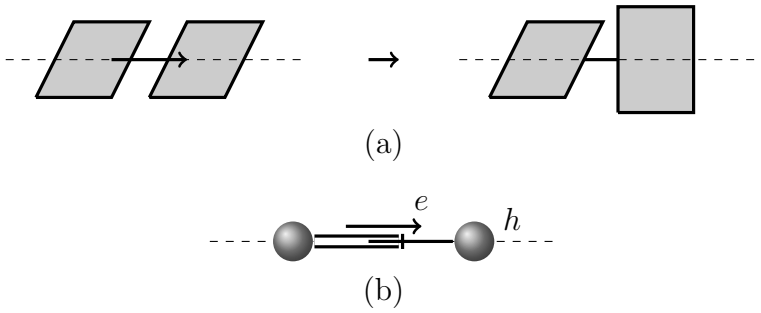

Figure 3: (a) A torsional hinge (with the dashed line denoting the hinge line). The vector indicates the directed edge e of the contact polyhedron. For a torsional hinge, the hinge line is collinear with the edge e. (b) A symbolic depiction of the torsional hinge, showing the hinge realised as a rod with a stop rotating within a cylindrical tube. Note that a torsional hinge in isolation has $\mathcal{D}_{\infty h}$ symmetry.

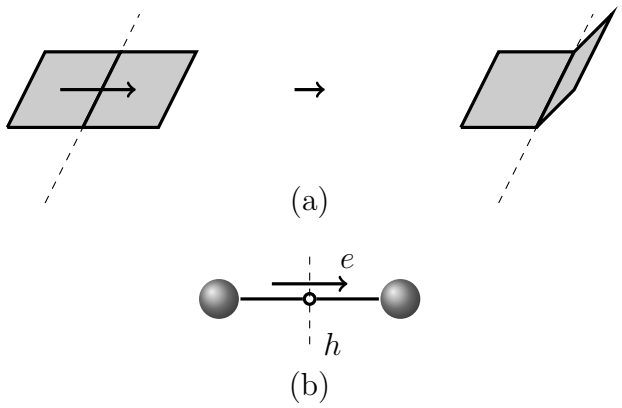

Figure 4: (a) A non-torsional hinge (with the dashed line denoting the hinge line). The vector indicates the directed edge e of the contact polyhedron. For a non-torsional hinge, the hinge line crosses the edge e. (b) A symbolic depiction of a non-torsional hinge. Note that a non-torsional hinge in isolation has at most $\mathcal{D}_{2h}$ symmetry, realised when the angle between e and h is 90°.

operation $x \in \mathcal{G}$ that leaves the hinge unshifted is χ_{revolute}, computed using the formula (Guest and Fowler, 2005):

$$\chi_{\text{revolute}}(x) = \chi_{R_h}(x)\chi_{e\|}(x).$$

The two terms on the RHS of this expression are easily computed and the results for χ_{revolute} are as shown in Tables 1 and 2 for torsional and non–torsional hinges, respectively.

	E	$C_n(h)$	C_2'	$\sigma(h\perp)$	$\sigma(h)$	i	$S_n(h)$
χ_{R_h}	1	1	−1	−1	1	1	1
$\chi_{e\|}$	1	1	−1	1	−1	−1	−1
χ_{revolute}	1	1	1	−1	−1	−1	−1

Table 1: Contribution to characters for a single torsional hinge that is unshifted under a given operation. C_2' are half-turns about axes perpendicular to the hinge line h. $\sigma(h\perp)$ is a mirror which contains the hinge line h. $\sigma(h)$ is the mirror with normal line h.

	E	$C_2(h)$	$C_2(e\|\|)$	$C_2(h\times e\|\|)$	i	$\sigma(h)$	$\sigma(e\|\|)$	$\sigma(h\times e\|\|)$
χ_{R_h}	1	1	−1	−1	1	1	−1	−1
$\chi_{e\|}$	1	−1	1	−1	−1	1	−1	1
χ_{revolute}	1	−1	−1	1	−1	1	1	−1

Table 2: Contribution to characters for a single non-torsional hinge that is unshifted under a given operation. $C_n(l)$ is the n-fold rotation about axis l: $C_2(e\|\|)$ is the two-fold rotation along the edge of the contact polyhedron; $C_2(h\times e\|\|)$ is the two-fold rotation about a line perpendicular to both the edge and the hinge line h. $\sigma(l)$ is the mirror with normal line l.

The characters of the representation $\Gamma(v, C)$, i.e., the permutation representation of the bodies, are used to construct the first line of Table 3. The following notation is used:

b is the number of bodies (number of vertices of the contact polyhedron C);

b_n denotes the number of vertices of C that are fixed by a rotation C_n, $n \geq 3$;

b_2 denotes the number of vertices of C that are fixed by a half-turn C_2;

b_σ denotes the number of vertices of C that are fixed by a reflection σ;

b_c denotes the number of vertices of C that are fixed by an inversion i;

b_{nc} denotes the number of vertices of C that are fixed by an improper rotation S_n, $n \geq 3$.

The characters of the representation $\Gamma_\parallel(e, C)$ are also used in the construction of the first line of Table 3. The relevant notation is:

e is the number of edges of the contact polyhedron C;

$e_\parallel$ is the number of edges which lie along a C_n axis (For $n > 2$ these edges must correspond to torsional hinges);

$e_\perp$ is the number of edges which lie perpendicular to a C_2 axis;

$e_{\parallel\sigma}$, $e_{\perp\sigma}$ are the numbers of edges that are centered in, and lie parallel / perpendicular to, a σ reflection plane;

e_c is the number of edges centered at the inversion centre;

e_{nc} is the number of edges that lie along an improper S_n rotation axis and are reversed by the S_n operation.

Finally, the characters of the representation $\Gamma_{\rm h}$ are given in the last line of Table 3. The relevant notation is:

$h = e$ is the number of hinges;

$h_{\parallel}^{(T)}$, $h_{\parallel}^{(NT)}$ are the numbers of torsional/non-torsional hinges whose hinge-line lies along the C_n axis ($n > 2$ is possible only for a torsional hinge);

$h_{\perp}^{(T)}$, $h_{\perp}^{(NT)}$ are the numbers of torsional/non-torsional hinges whose hinge-line lies across a C_n axis (only $n = 2$ is possible);

$h_{\parallel\sigma}^{(T)}$, $h_{\perp\sigma}^{(T)}$, $h_{\parallel\sigma}^{(NT)}$, $h_{\perp\sigma}^{(NT)}$ are the numbers of torsional/non-torsional hinges centered in, and lying parallel/perpendicular to, a σ reflection plane;

$h_c^{(T)}$, $h_c^{(NT)}$ are the numbers of torsional/non-torsional hinges whose hinge-lines are centered at the inversion centre;

$h_{nc}^{(T)}$ is the number of torsional hinges whose hinge-line lies along an S_n axis where $n > 2$, and are reversed by the S_n operation (possible only for a torsional hinge).

	E	$C_{n\neq 2}(\phi)$	C_2	σ	i	$S_{n\neq 2}(\phi)$
$\Gamma(v,C)-\Gamma_{\parallel}(e,C)-\Gamma_0$	$b-e-1$	$b_n-e_{\parallel}-1$	$b_2+e_{\perp}-e_{\parallel}-1$	$b_{\sigma}+e_{\perp\sigma}-e_{\parallel\sigma}-1$	b_c+e_c-1	$b_{nc}+e_{nc}-1$
$\Gamma_T+\Gamma_R$	6	$4\cos\phi+2$	-2	0	0	0
Γ_{h}	h	$h_{\parallel}^{(T)}$	$h_{\parallel}^{(T)}+h_{\perp}^{(T)}+$ $h_{\perp}^{(NT)}-h_{\parallel}^{(NT)}$	$-h_{\parallel\sigma}^{(T)}-h_{\perp\sigma}^{(T)}-$ $h_{\parallel\sigma}^{(NT)}+h_{\perp\sigma}^{(NT)}$	$-h_c^{(T)}-h_c^{(NT)}$	$-h_{nc}^{(T)}$

Table 3: Calculations of representations used in the symmetry-extended mobility rule for body-hinge structures. The table applies to three-dimensional frameworks; the restriction to two dimensions is achieved by deleting columns i and $S_{n\neq 2}(\phi)$, setting all $h^{(T)}$ quantities to zero, and setting the first three entries in $\Gamma_T+\Gamma_R$ to 3, $2\cos\phi+1$ and -1, respectively.

5. Examples

By Tay's theorem (Tay, 1984) and the proof of the molecular conjecture (Katoh and Tanigawa, 2011), a generic body-hinge or molecular framework in three dimensions with b bodies and h hinges is isostatic if and only if it satisfies the scalar count $5h = 6b - 6$, and for all substructures with h' hinges connecting b' bodies, we have $5h' \leq 6b' - 6$. In the following, we use the symmetry representations of the previous section to examine the symmetry-induced mobility of some symmetric body-hinge structures which are predicted to be isostatic by Tay's counts.

5.1. Conformers of cyclohexane

As a first example, we consider a ring of six carbon atoms (the carbon skeleton of the cyclohexane molecule) and its two basic conformations, the 'boat' and the 'chair' (see Figure 5.1). These structures are also *molecular frameworks* in the mathematical sense, consisting of six bodies (atoms) and six torsional hinges (bonds). Clearly, cyclohexane satisfies the isostatic scalar count $5h = 6b - 6 = 30$, and it is easy to verify that the sparsity condition for all substructures is also satisfied. Thus, generic realisations of this 6-loop Guest and Fowler (2010) framework are isostatic.

Suppose now that the structure is realised with $\mathcal{C}_2$ symmetry, as the *boat* conformation of cyclohexane (see Figure 5.1(a)). As there is no hinge fixed by the half-turn, it follows from the characters in Table 3 that there must be exactly one body fixed by the half-turn (i.e., $b_2 = 1$) for the structure to

be isostatic. Thus, since the boat conformation has no body fixed by the half-turn, we may conclude that the boat is not isostatic. In fact, we have $\Gamma(m)-\Gamma(s) = A-B$, as computed in (Guest and Fowler, 2010), for example, and there is a well known continuous mechanism between boat forms (see e.g., Graveron-Demilly (1977, 1978)).

Similarly, using the calculations in Table 3, it is easy to verify that the chair conformation of cyclohexane (i.e., the six-ring realised with $\mathcal{C}_3$ symmetry) satisfies the count $\Gamma(m) - \Gamma(s) = 0$, as there is neither a hinge nor a body fixed by the three-fold rotation (see Figure 5.1(b)). Thus, the 'chair' is correctly predicted to be isostatic.

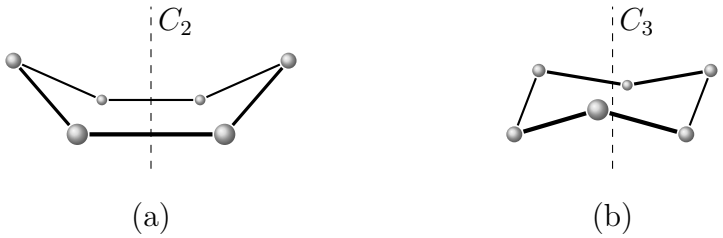

Figure 5: Two basic conformations of cyclohexane: The 'boat' has half-turn symmetry and is flexible (a); the 'chair' has 3-fold rotational symmetry and is isostatic (b).

The $\mathcal{C}_2$-preserving continuous mechanism of the 'boat' and the rigidity of the 'chair' were also treated in (Schulze et al., 2013) by modeling the molecular structures as body-bar frameworks, where each hinge is replaced by 5 independent bars, each intersecting the corresponding hinge line (leaving one relative degree of freedom between a pair of bodies), and by applying 'orbit counting methods' (Schulze et al., 2013; Schulze and Whiteley, 2011; Tanigawa, 2012) for body-bar frameworks to these structures.

However, note that while the orbit counts in (Schulze et al., 2013) (as well as the results in (Guest et al., 2010) and (Tanigawa, 2012)) provide information about the (symmetry-preserving) mobility of symmetric *body-bar* realisations of a given multi-graph, a proof of the symmetric version of the molecular conjecture would be needed to transfer these results to symmetric *molecular* realisations of the multi-graph. More precisely, the *symmetric molecular conjecture* asserts that under symmetry-generic conditions, a body-bar framework and a molecular framework with the same underlying multi-graph have the same rigidity properties (Porta et al., 2013); that is, the special geometry of the positioning of the hinge lines in a symmetry-generic molecular realisation of the multi-graph cannot give rise to any additional (first-order) flexibility.

As the special geometry of the hinge locations in a molecular framework is captured by the contact polyhedron C, the present method allows us to analyze the mobility of symmetric molecular structures directly, without using the unproven symmetric molecular conjecture, and hence is more powerful than orbit-based counting methods for body-bar frameworks. In fact, part of the motivation for the present contribution is that our results concerning the rigidity and flexibility of symmetric body-hinge and molecular frameworks can be compared with corresponding results for symmetric body-bar frameworks in order to probe the symmetric molecular conjecture. For example, when compared with the symmetry counts for body-bar frameworks derived in (Guest et al., 2010), the symmetry counts for the corresponding molecular

frameworks obtained in this paper do not give rise to any added necessary conditions for rigidity, and are thus compatible with the symmetric molecular conjecture.

5.2. Ring of rotating tetrahedra

Another symmetric body-hinge structure with the 6-cycle as a contact graph is the ring of six rotating tetrahedra shown in Figure 6. The maximal symmetry that this structure can achieve is $\mathcal{D}_{3d}$. Note that the positioning of the hinge lines in this structure prevents us from choosing a contact polyhedron with $\mathcal{D}_{3d}$ symmetry whose edges are aligned with the hinge lines. Therefore, each of the hinges in this structure is non-torsional. For each reflection σ with a 'vertical mirror plane' in the group, there are exactly two hinges that are fixed by σ, and since both of these hinges lie parallel to the reflection plane (i.e., $h_{\|\sigma}^{(NT)} = 2$), the characters in Table 3 imply that the structure has a non-trivial first-order motion. In fact, this motion extends to a continuous mechanism which maintains $\mathcal{C}_{3v}$ symmetry throughout the path. For a detailed analysis of this mechanism we refer the reader to (Guest, 2000; Fowler and Guest, 2005; Guest and Fowler, 2010).

5.3. A partial prism

Next, we consider the molecular structure shown in Figure 7. This structure is based on a partial octagonal prism and consists of two rings of 8 bodies alternating with (8) torsional hinges which are linked by two additional torsional hinges. This structure is easily verified to satisfy the non-symmetric

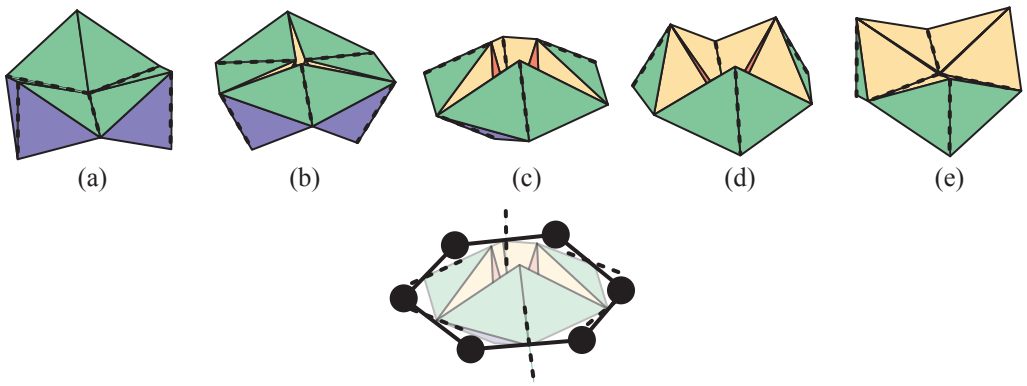

Figure 6: The finite motion of the rotating ring of six tetrahedra, showing one quarter of a complete cycle: (a) D_{3h} high symmetry point; (b) generic C_{3v} symmetry; (c) D_{3d} high symmetry point; (d) generic C_{3v} symmetry; (e) D_{3h} high symmetry point. The hinge lines between tetrahedra have been marked with a dashed line. The contact polyhedron is also shown for (c), where the edges of the polyhedron are perpendicular to the hinge lines, which are shown dashed and centred on the polyhedron edges.

Tay counts, and hence is isostatic for generic, non-symmetric realisations. As indicated in Figure 7, the structure can be realised with a maximal point group symmetry of $\mathcal{D}_{2h}$, in which case it follows immediately from the characters in Table 3 that there exists a non-trivial first-order motion. Since two of the three half-turn axes intersect neither a body nor hinge, the structure cannot be isostatic. In Table 4, we give a detailed analysis of $\mathcal{D}_2$-symmetric realisations of this structure using the symmetry-extended mobility rule.

By the computation shown in Table 4, we have $\Gamma(m) - \Gamma(s) = A_1 - B_2$, indicating one mechanism that preserves the full $\mathcal{D}_2$ symmetry, and a B_2-symmetric state of self-stress that is symmetric under only one of the two-fold rotations. As the mechanism is totally symmetric and the state of self-stress is not, the mechanism is finite (Kangwai and Guest, 1999; Guest and Fowler,

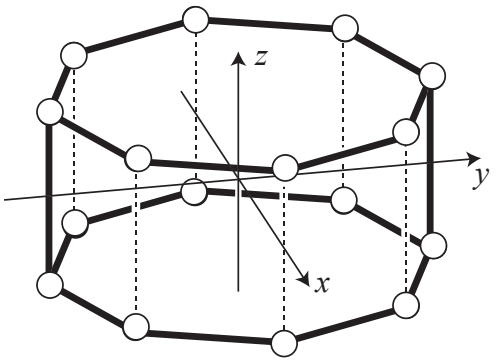

Figure 7: A molecular structure based on a partial octagonal prism which has a continuous motion that preserves $\mathcal{D}_2$ symmetry. Dashed lines indicate edges that are removed from the complete prism to form this structure. Axes x, y and z are C_2 symmetry elements.

$\mathcal{D}_2$	E	$C_2(x)$	$C_2(y)$	$C_2(z)$
$\Gamma(v,C)$	16	0	0	0
$-\Gamma_{\parallel}(e,C)$	−18	0	2	0
$-\Gamma_0$	−1	−1	−1	−1
$=$	−3	−1	1	−1
$\times(\Gamma_T+\Gamma_R)$	6	−2	−2	−2
$=$	−18	2	−2	2
$+\Gamma_{\mathrm{h}}$	18	0	2	0
$=\Gamma(m)-\Gamma(s)$	0	2	0	2

Table 4: Calculation of representations used in the symmetry-extended mobility rule for the molecular structure shown in Figure 7, and here analysed in $\mathcal{D}_2$ symmetry.

2007) (see also (Schulze, 2010)).

In Porta et al. (2013), orbit-counting methods for symmetric *body-bar* frameworks were used to predict a symmetry-preserving continuous mechanism of this structure whenever it is realised with $\mathcal{D}_2$ (or $\mathcal{C}_2$) point group symmetry. To gather evidence for the symmetric version of the molecular conjecture, the configuration spaces of the corresponding *molecular* structures were then computed, which confirmed that the special geometry of the disposition of the hinges in $\mathcal{D}_2$-generic (or $\mathcal{C}_2$-generic) molecular realisations of the structure does not give rise to any added flexibility.

Using the constructions to be described in Section 7, we can easily generate further examples of molecular frameworks with various point-group symmetries and possessing a small number of symmetry-induced mechanisms. These structures lend themselves to additional testing of their configuration spaces in order to investigate further the symmetric molecular conjecture.

5.4. Further examples

Finally, consider the body-hinge structure with $\mathcal{C}_3$ symmetry depicted in Figure 8. The hinges of this structure are all non-torsional. If analysed in $\mathcal{C}_3$ symmetry, the structure satisfies the symmetry-extended mobility rule: for a 3-fold rotation, there is no restriction on the number of bodies that lie on the rotational axis. The corresponding detailed symmetry analysis is given in Table 5. It follows from these computations that $\Gamma(m) - \Gamma(s) = 0$. However, if we realise this structure with $\mathcal{C}_{3v}$ symmetry, then it cannot be isostatic,

$\mathcal{C}_3$	E	C_3	C_3^2
$\Gamma(v,C)$	11	2	2
$-\Gamma_{\parallel}(e,C)$	-12	0	0
$-\Gamma_0$	-1	-1	-1
$=$	-2	1	1
$\times(\Gamma_T+\Gamma_R)$	6	0	0
$=$	-12	0	0
$+\Gamma_{\mathrm{h}}$	12	0	0
$=\Gamma(m)-\Gamma(s)$	0	0	0

Table 5: Calculation of representations used in the symmetry-extended mobility rule for the $\mathcal{C}_3$-symmetric body-hinge structure shown in Figure 8.

since for each reflection σ in the group, we then have $h^{(NT)}_{\parallel\sigma} = 0 \neq 4 = h^{(NT)}_{\perp\sigma}$. The corresponding detailed computation for the symmetry-extended mobility rule for the group $\mathcal{C}_{3v}$ is shown in Table 6.

Note that it follows from these calculations that $\Gamma(m) - \Gamma(s) = 2A_1 - 2A_2$, which implies that there are two fully symmetric (A_1) non-trivial degrees of freedom and two states of self-stress of symmetry A_2 (symmetric under rotation, but antisymmetric under reflection). Thus, by the results in (Kangwai and Guest, 1999; Guest and Fowler, 2007; Schulze, 2010), we may conclude that the structure has in fact two *continuous* symmetry preserving mechanisms.

6. General symmetry conditions for isostatic behaviour

From Table 3, the symmetry treatment of the body-hinge mobility rule in 3-space reduces to scalar equations of six types. If $\Gamma(m) - \Gamma(s) = 0$, then

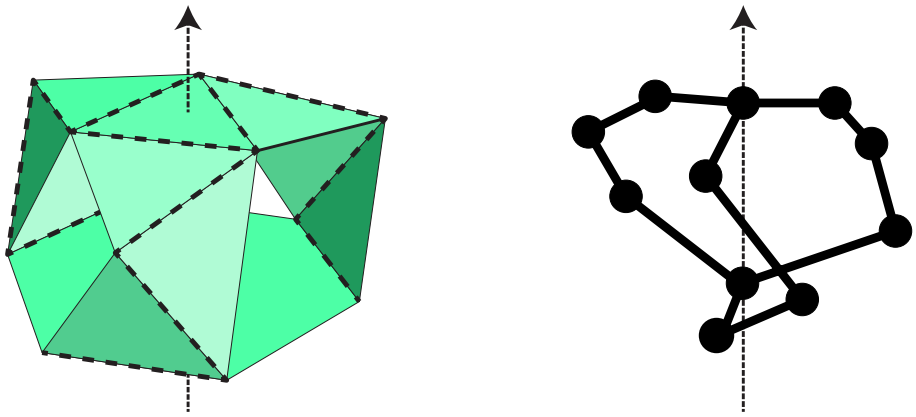

Figure 8: (a) A body-hinge structure with C_3 symmetry, where each body is a flat panel. The hinge lines between panels are marked with a dashed line, and the C_3 axis is indicated by an arrow. (b) The contact polyhedron.

$\mathcal{C}_{3v}$	E	$2C_3$	$3\sigma_v$
$\Gamma(v,C)$	11	2	5
$-\Gamma_{\parallel}(e,C)$	−12	0	−4
$-\Gamma_0$	−1	−1	−1
$=$	−2	1	0
$\times(\Gamma_T+\Gamma_R)$	6	0	0
$=$	−12	0	0
$+\Gamma_{\mathrm{h}}$	12	0	4
$=\Gamma(m)-\Gamma(s)$	0	0	4

Table 6: Calculation of representations used in the symmetry-extended mobility rule for $\mathcal{C}_{3v}$-symmetric realisations of the body-hinge structure shown in Figure 8.

(i) $E : 6b - 6 = 5h$ (recall $e = h$)

(ii) $C_{n\neq 2}(\phi) : (4\cos\phi + 2)(b_n - h_{\parallel}^{(T)} - 1) + h_{\parallel}^{(T)} = 0$ (all hinges on an axis with $n > 2$ must be torsional hinges)

(iii) $C_2 : h_{\parallel}^{(T)} + h_{\perp}^{(T)} + h_{\perp}^{(NT)} - h_{\parallel}^{(NT)} = 2(b_2 - e_{\parallel} + e_{\perp} - 1)$

(iv) $\sigma : h_{\perp\sigma}^{(NT)} - h_{\parallel\sigma}^{(NT)} = h_{\parallel\sigma}^{(T)} + h_{\perp\sigma}^{(T)}$

(v) $i : h_c^{(T)} + h_c^{(NT)} = 0$

(vi) $S_{n\neq 2}(\phi) : h_{nc}^{(T)} = 0$

Hence, some observations and *necessary* conditions for isostatic behaviour are:

C_2 If there is no fixed hinge, then we need exactly one fixed body.

$C_{n\neq 2}$ We note that the function $(4\cos\phi + 2)$, with $\phi = 2\pi/n$, takes integer values for $n = 1, 2, 3, 4, 6$. If n is not one of these values (i.e., 5, 7 or above) then $h_{\parallel}^{(T)} = 0$ and $b_n = 1$ is the only solution.

C_3 We must have $h_{\parallel}^{(T)} = 0$, but there is no restriction on the number of bodies on the axis, b_3.

C_4 For $n = 4$ the equation reduces to $2(b_4 - 1) = h_{\parallel}^{(T)}$, and hence $h_{\parallel}^{(T)}$ is clearly even. However the solutions for $h_{\parallel}^{(T)} = 2$ and 4 imply that the skeleton of C is a multigraph and so are not allowed. Note that $b_4 = 1$, $h_{\parallel}^{(T)} = 0$ is a viable solution.

C_6 For $n = 6$ the equation reduces to $4(b_6 - 1) = 3h_{\parallel}^{(T)}$. Clearly $b_6 = 1$, $h_{\parallel}^{(T)} = 0$ is a viable solution.

i and $S_{n\neq 2}$ No hinge can be unshifted by any improper operation.

Useful simplified conditions arise for body-hinge structures restricted to only torsional or only non-torsional hinge types, where these can be constructed. (Symmetry may dictate the types of some symmetrically placed hinges in a structure and render one or both of the pure framework types impossible.) For frameworks with only torsional hinges, we have $e = h^{(T)}$, $e_{\parallel} = h_{\parallel}^{(T)}$ and $e_{\perp} = h_{\perp}^{(T)}$, giving:

T(iii) $C_2 : 2(b_2 - 1) = 3h_{\parallel}^{(T)} - h_{\perp}^{(T)}$

T(iv) $\sigma : h_{\parallel\sigma}^{(T)} + h_{\perp\sigma}^{(T)} = 0$

Hence, some additional conditions for isostatic behaviour of *molecular* structures are:

C_2 Some viable solutions are: (i) $b_2 = 0$, $h_{\parallel}^{(T)} = 0$, $h_{\perp}^{(T)} = 2$; (ii) $b_2 = 1$ if and only if $h_{\parallel}^{(T)} = h_{\perp}^{(T)} = 0$; (iii) $b_2 = 2$, $h_{\parallel}^{(T)} = h_{\perp}^{(T)} = 1$.

σ, i and $S_{n\neq 2}$ No hinge can be unshifted by any improper operation.

For frameworks with only non-torsional hinges, we have $e = h^{(NT)}$, but cannot give direct relationships between $e_{\parallel}, e_{\perp}$ and $h_{\parallel}^{(NT)}, h_{\perp}^{(NT)}$, as for an edge of C perpendicular to a symmetry axis, the hinge line may be either parallel or perpendicular to the symmetry axis.

NHT (i): $6b - 6 = 5h^{(NT)}$

NCT$_{n\neq 2}$ (ii): $(4\cos\phi + 2)(b_n - 1) = 0$

NCT$_2$ (iii): $h_{\perp}^{(NT)} - h_{\parallel}^{(NT)} = 2(b_2 - e_{\parallel} + e_{\perp} - 1)$

NST (iv): $h_{\perp\sigma}^{(NT)} = h_{\parallel\sigma}^{(NT)}$

NVT (v): $h_{\sigma}^{(NT)} = 0$

NST$_{n\neq 2}$ (vi): $(\phi) : 0 = 0$

Hence, some further conditions for isostatic behaviour of frameworks with only non-torsional hinges are:

$C_{n\neq 3}$ $b_n = 1$ for all $n > 2$.

A direct consequence of the above conditions is that we can construct an isostatic body-hinge framework exhibiting any desired point group symmetry $\mathcal{G}$. The recipe is as follows: Take one central body and attach a loop of five additional bodies connected by six hinges in general position to give an isostatic ring. Then use the $|\mathcal{G}|$ operations of the group to copy the additional bodies and hinges to give a final framework consisting of a central body decorated with a regular orbit of isostatic rings. The whole structure has $1+5|\mathcal{G}|$ bodies and $6|\mathcal{G}|$ hinges, with $\Gamma(v, C) = \Gamma_0 + 5\Gamma_{\rm reg}$ and $\Gamma_{\parallel}(e, C) = \Gamma_{\rm h} = 6\Gamma_{\rm reg}$ (where $\Gamma_{\rm reg}$ has character $|\mathcal{G}|$ under the identity, and zero under all other symmetry operations), giving $\Gamma(m) - \Gamma(s) = 0$, and confirming that this bouquet-like structure is isostatic overall.

In 2D, where all hinges are non-torsional and all hinge lines are perpendicular to the corresponding edge of C, the possible point groups $\mathcal{C}_{nv}$ (and their $\mathcal{C}_s$ or $\mathcal{C}_n$ subgroups) imply four symmetry conditions:

2D (i) $3b - 3 = 2h$

2D (ii) $D_{k\neq 2}(\phi) : (2\cos\phi + 1)(b_n - 1) = 0$

2D (iii) $h = 2(b_2 - e_{\|} + e_{\perp} - 1)$

2D (iv) $h_{\perp\sigma} = h_{\|\sigma}$

with the consequence that $b_n = 1$ for all C_n with $n > 3$.

7. Constructing symmetric body-hinge structures with isostatic counts

Suppose, for a loopless multi-graph with v vertices and e edges, we replace each vertex by a body and each edge by a chain of $k \geq 1$ bodies and $k + 1$ hinges. Then we obtain a body-hinge structure with $b = v + ke$ bodies and $h = (k+1)e$ hinges. We call this process '*k-expansion*'. We are interested in structures with the (3D) isostatic count $6b - 6 = 5h$, that is,

$$\begin{aligned} 6(v + ke) - 6 &= 5(k+1)e \\ 6(v-1) &= (5-k)e. \end{aligned}$$

We distinguish the following four cases:

(i) $k = 1$. Then we have $e = \frac{3}{2}(v - 1)$.

(ii) $k = 2$. Then we have $e = 2(v - 1)$.

(iii) $k = 3$. Then we have $e = 3(v - 1)$.

(iv) $k = 4$. Then we have $e = 6(v - 1)$.

Note that in order to obtain isostatic body-hinge structures, the starting multi-graph must satisfy one of the above overall counting conditions for e and v, and also the corresponding sparsity counts for all subgraphs. For example, for $k = 2$, we must have the overall count $e = 2(v - 1)$, and the count $e' \leq 2(v' - 1)$ for each subgraph.

7.1. Case (i)

If $k = 1$, then v must clearly be odd. Also, the starting graph on which we perform the expansion cannot have multiple edges, for otherwise the expanded contact graph would contain a 4-cycle, and hence the corresponding body-hinge structure would not be isostatic. Loops are not allowed: as we are replacing a loop edge by a chain of k bodies and $k + 1$ hinges, and $k \in \{1, 2, 3, 4\}$, a loop gives rise to a K-ring in the body-hinge structure with $K \in \{2, 3, 4, 5\}$, and hence leads to an over-braced substructure (or in the case of $k = 1, K = 2$, a non-valid body-hinge structure). Thus, the smallest non-trivial starting graph is the complete graph K_3 which on expansion becomes the contact graph of a ring of six bodies alternating with hinges.

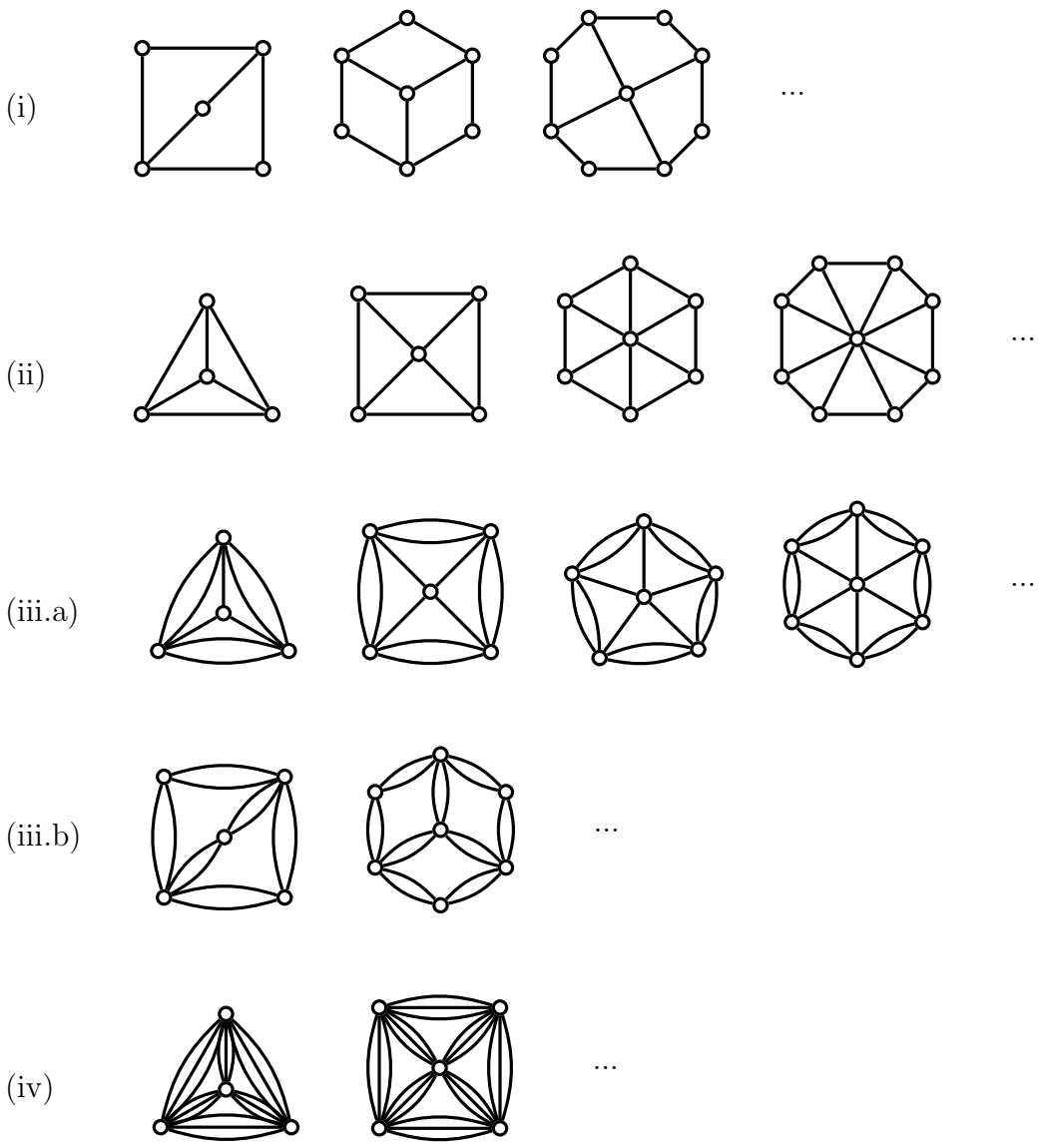

Figure 9: Infinite families of graphs whose k-expansions are contact graphs of body-hinge structures which satisfy the 3D isostatic count. If these structures are realised with certain point group symmetries, then they also satisfy the added symmetry conditions for isostatic character derived in Sections 4 and 6.

An infinite family of graphs which satisfy both the overall count $e = \frac{3}{2}(v-1)$ and the sparsity count $e' = \frac{3}{2}(v'-1)$ for all subgraphs are the 'partial wheels' $W_{2n}^{(\text{part})}$ depicted in Figure 9 (i). If the corresponding body-hinge structures are realised with $\mathcal{C}_n$ symmetry so that the n-fold rotation fixes the central body, but shifts all other bodies and hinges, then the structure also satisfies the symmetry conditions for isostatic character derived in Section 6.

Similarly, if a body-hinge structure has a 1-expansion of a partial wheel $W_{4n}^{(\text{part})}$, $n \geq 1$, as its contact graph, and if it is realised with $\mathcal{C}_i$ symmetry, where the central body is fixed by the inversion, then the symmetry condition for the inversion given in Section 6 is also satisfied.

However, in general, for other types of symmetric body-hinge frameworks which are constructed from a 1-expansion of a partial wheel $W_{2n}^{(\text{part})}$, our symmetry conditions detect a non-trivial first-order motion.

Note that if we start with a graph that satisfies the count $e = \frac{3}{2}(v-1)$, then we can always add two vertices and three edges to retain the isostatic count, as illustrated in Figure 10. This allows us to generate large structures which satisfy the isostatic scalar counts, and which can easily be examined for flexibility using the symmetry extended mobility rule.

7.2. Case (ii)

In this case, the starting graph is allowed to have multiple edges, but no loops. If we start with a multi-graph that satisfies the count $e = 2(v-1)$, we can perform any 2-dimensional Henneberg-type graph construction (such

Figure 10: For any starting graph satisfying the count $e = \frac{3}{2}(v-1)$, we can add two vertices and three edges to retain the isostatic count, bridging any pair of vertices of the original graph (a). Alternatively, we can 'add a triangle' to the original graph, which in the expanded graph, is equivalent to adding a six-ring (b).

as a vertex 2-addition, an edge 2-split or an X-replacement, e.g. (Tay and Whiteley, 1985; Ross and Nixon, 2012)) on the graph to retain the isostatic count. By performing these constructions symmetrically, we may obtain many symmetric contact graphs of body-hinge structures which have isostatic counts. Clearly, some modified constructions which add multiple edges to the graph are also permitted. Further, the count $e = 2(v-1)$ implies that if we take the graph of any 2-dimensional rigidity circuit, replace each vertex by a body, and each edge by 2 bodies and 3 hinges, then we obtain a body-hinge structure that has an isostatic count. So, in particular, we may also use 2D circuit-gluing to obtain new structures (Ross and Nixon, 2012).

Note that the wheel graphs W_n shown in Figure 9 (ii) correspond to body-hinge structures which also satisfy the extra symmetry conditions derived in Section 6 for the groups $\mathcal{C}_n$, provided that the n-fold rotation fixes the central body and shifts all other bodies and hinges. Similarly, for W_{2n}, the corresponding body-hinge structure satisfies the symmetry condition for $\mathcal{C}_i$, if the central body is fixed by the inversion.

It may be interesting to note that the count $e = 2(v-1)$ is satisfied by all

self-dual polyhedra, e.g., the pyramids (whose skeletons are the wheel graphs) and towers constructed by topping a stack of $[N]$-prisms with an $[N]$-pyramid. A tower of an $[N]$-pyramid topping p $[N]$-prisms has $v = 1 + (p + 1)N$ and $e = 2(p+1)N$ and after decoration with 2 bodies and 3 hinges per edge, the body and hinge counts are respectively $b = 1+5(p+1)N$, and $h = 6(p+1)N$. By counting, the characters of $\Gamma(m) - \Gamma(s)$ corresponding to the identity E and the rotations $C_{n\neq 2}$ are 0, since $b_n = 1$. Hence, in $\mathcal{C}_n$, $\Gamma(m) - \Gamma(s) = 0$ and there are no symmetry-detectable mechanisms or states of self stress.

7.3. Case (iii)

The smallest non-trivial example in this case is the graph with two vertices which are connected by three parallel edges. This gives rise to the structure discussed in Section 5 and shown in Fig. 8. In general, if we start with a loopless multi-graph that satisfies the count $e = 3(v - 1)$, then we can perform any 3-dimensional Henneberg-type graph construction (such as a vertex 3-addition or edge 3-split, e.g. (Ross and Nixon, 2012)) to preserve this count. Clearly, as in Case (ii), some modified constructions which add multiple edges to the graph are again permitted.

Note that 2-expansions of the wheel graphs with doubled outer edges shown in Figure 9 (iii.a) (denoted by $W_n^{(\text{double})}$) and 2-expansions of the partial wheel graphs with all edges doubled shown in Figure 9 (iii.b) (denoted by $2W_{2n}^{(\text{part})}$) can be realised as symmetric body-hinge structures that satisfy the symmetry conditions derived in Section 6, for a number of point groups.

For example, each of these structures can clearly be realised with $\mathcal{C}_n$ symmetry so that there is exactly one body (the central body) and no hinge fixed by the n-fold rotation. Further, the symmetry extended counts for the groups $\mathcal{D}_n$ and $\mathcal{S}_{2n}$ can be satisfied for appropriate realisations of 2-expanded wheel graphs $W_{2n}^{(\text{double})}$, and the symmetry extended counts for the groups $\mathcal{C}_{nv}$, $\mathcal{C}_s$ and $\mathcal{D}_{nh}$ can be satisfied for appropriate realisations of 2-expanded partial wheel graphs $2W_{2n}^{(\text{part})}$.

7.4. Case (iv)

In this case, we can again use similar constructions as above to generate large body-hinge structures which satisfy the non-symmetric Tay counts, as well as the added symmetry conditions for various point groups. For example, an infinite family of such structures is obtained from 4-expansions of wheel graphs whose edges are all tripled, as illustrated in Figure 9 (iv). A 4-expansion of the graph $3W_3$ (where $3W_3$ is obtained from the simple wheel graph W_3 by replacing each edge with a set of three parallel edges) for example, can be realised as a molecular framework with point group $\mathcal{T}$ (i.e., with the purely rotational symmetry group of a regular tetrahedron) so that the criteria of the symmetry extended mobility rule are all satisfied.

7.5. Further Constructions

Finally, we note that there are many other constructions for body-hinge structures with isostatic scalar counts. For example, if we start with the contact graph based on a partial octagonal prism shown in Figure 11 (a),

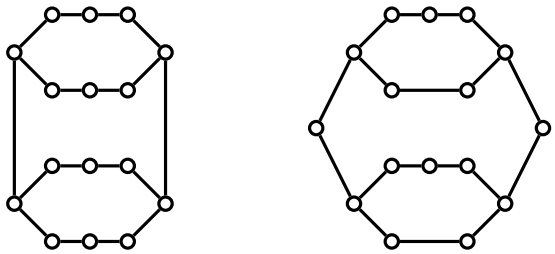

(a) (b)

Figure 11: Contact graphs of body-hinge structures (where each vertex represents a body and each edge represents a hinge) which correspond to 'partial prisms'. The graph in (a) is the contact graph of the structure shown in Figure 7.

reduce each of the two 8-cycles to 7-cycles, and replace both of the vertical edges by a path of two edges, then the isostatic counts are preserved (see Figure 11 (b)). Alternatively, we could expand the two cycles on the top and on the bottom and add an appropriate number of vertical bars linking the two rings to preserve the isostatic counts. If realised with certain point group symmetries, these structures also satisfy the symmetry conditions derived in Section 6.

References

Altmann, S. L. and Herzig, P. (1994). *Point-Group Theory Tables*. Clarendon Press, Oxford.

Atkins, P. W., Child, M. S., and Phillips, C. S. G. (1970). *Tables for Group Theory*. Oxford University Press.

Baker, D. and Friswell, M. I. (2009). Determinate structures for wing camber control. *Smart Materials and Structures*, 18(3):035014.

Bishop, D. M. (1973). *Group Theory and Chemistry*. Clarendon Press, Oxford.

Bujakas, V. J. and Rybakova, A. G. (1998). High precision deployment and shape correction of multimirror space designs. In Pellegrino, S. and Guest, S. D., editors, *IUTAM-IASS Symposium on Deployable Structures: Theory and Applications*, pages 55–62. Kluwer Academic Publishers.

Calladine, C. R. (1978). Buckminster Fuller's "Tensegrity" structures and Clerk Maxwell's rules for the construction of stiff frames. *International Journal of Solids and Structures*, 14:161–172.

Chen, Y., Guest, S., Fowler, P., and Feng, J. (2012). Two-orbit switch-pitch structures. *Journal of the International Association for Shell and Spatial Structures*, 53:157–162.

Connelly, R., Fowler, P. W., Guest, S. D., Schulze, B., and Whiteley, W. J. (2009). When is a symmetric pin-jointed framework isostatic? *International Journal of Solids and Structures*, 46:762–773.

Cotton, F. A. (1990). *Chemical Applications of Group Theory*. John Wiley & Sons, New York.

Fowler, P., Guest, S., and Schulze, B. (2014). Mobility in symmetry-regular bar-and-joint frameworks. *Fields Institute Proceedings, to appear*.

Fowler, P. W. and Guest, S. D. (2000). A symmetry extension of Maxwell's rule for rigidity of frames. *International Journal of Solids and Structures*, 37:1793–1804.

Fowler, P. W. and Guest, S. D. (2005). A symmetry analysis of mechanisms in rotating rings of tetrahedra. *Proceedings of the Royal Society: Mathematical, Physical & Engineering Sciences*, 461:1829–1846.

Graveron-Demilly, D. (1977). Conformation maps of some saturated six and seven membered rings. *Journal of Chemical Physics*, 66:2874–2877. See also Graveron-Demilly (1978).

Graveron-Demilly, D. (1978). Erratum: Conformational maps of some saturated six and seven membered rings. *Journal of Chemical Physics*, 68:785.

Guest, S. and Pellegrino, S. (1994). The folding of triangulated cylinders, part ii: The folding process. *ASME Journal of Applied Mechanics*, 61:777–783.

Guest, S., Schulze, B., and Whiteley, W. (2010). When is a body-bar structure isostatic? *International Journal of Solids and Structures*, 47:2745–2754.

Guest, S. D. (2000). Tensegrities and rotating rings of tetrahedra: a symmetry viewpoint of structural mechanics. *Philosophical Transactions of the Royal Society of London*, 358(358):229–243.

Guest, S. D. and Fowler, P. W. (2005). A symmetry-extended mobility rule. *Mechanism and Machine Theory*, 40:1002–1014.

Guest, S. D. and Fowler, P. W. (2007). Symmetry conditions and finite mechanisms. *Journal of Mechanics of Materials and Structures*, 2(2):293–301.

Guest, S. D. and Fowler, P. W. (2010). Mobility of 'N-loops'; bodies cyclically connected by intersecting revolute hinges. *Proceedings of the Royal Society A: Mathematical, Physical and Engineering Science*, 466:63–77.

Hunt, K. H. (1978). *Kinematic Geometry of Mechanisms*. Clarendon Press, Oxford.

James, G. D. and Liebeck, M. W. (2001). *Representations and Characters of Groups*. Cambridge University Press.

Kangwai, R. D. and Guest, S. D. (1999). Detection of finite mechanisms in symmetric structures. *International Journal of Solids and Structures*, 36(36):5507–5527.

Katoh, N. and Tanigawa, S. (2011). A proof of the molecular conjecture. *Discrete & Computational Geometry*, 45(4):647–700.

Maxwell, J. C. (1864). On the calculation of the equilibrium and stiffness of frames. *Philosophical Magazine.*, 27:294–299.

Maxwell, J. C. (1876). General considerations concerning scientific apparatus. In *South Kensington Museum Handbook to the Special Loan Collection of Scientific Apparatus*. Chapman and Hall.

Miura, K., Furuya, H., and Suzuki, K. (1985). Variable geometry truss and its application to deployable truss and space crane arm. *Acta Astronautica*, 12(7–8):599–607.

Porta, J., Ros, L., Schulze, B., Sljoka, A., and Whiteley, W. (2013). On the symmetric molecular conjectures. *to appear in Proc. Computational Kinematics*.

Röschel, O. (2002). Und sie bewegen sich doch – neue übergeschlossene Polyedermodelle. *Informationsblätter der Geometrie (IBDG)*, 1:37–41.

Röschel, O. (2012). A fulleroid-like mechanism based on the cube. *Journal for geometry and graphics*, 16:19–27.

Ross, E. and Nixon, T. (2012). One brick at a time: a survey of inductive constructions in rigidity theory. arXiv:1203.6623.

Schulze, B. (2010). Symmetry as a sufficient condition for a finite flex. *SIAM Journal on Discrete Mathematics*, 24(4):1291–1312.

Schulze, B., Sljoka, A., and Whiteley, W. (2013). How does symmetry impact the flexibility of proteins? *to appear in Phil. Trans. Royal Soc. A*.

Schulze, B. and Whiteley, W. (2011). The orbit rigidity matrix of a symmetric framework. *Discrete & Computational Geometry*, 46(3):561–598.

Stewart, D. (1965). A platform with six degrees of freedom. *Proceedings of the Institution of Mechanical Engineers*, 180(1):371–386.

Tanigawa, S. (2012). Matroids of gain graphs in Applied Discrete Geometry. arXiv:1207.3601.

Tay, T. (1984). Rigidity of multi-graphs, linking rigid bodies in n-space. *J. Comb. Theory, B*, 36:95–112.

Tay, T. and Whiteley, W. (1984). Recent advances in the generic rigidity of structures. *Structural Topology*, 9:31–38.

Tay, T. and Whiteley, W. (1985). Generating isostatic frameworks. *Structural Topology*, 11:21–29.